Nanoscale

Accepted Manuscript

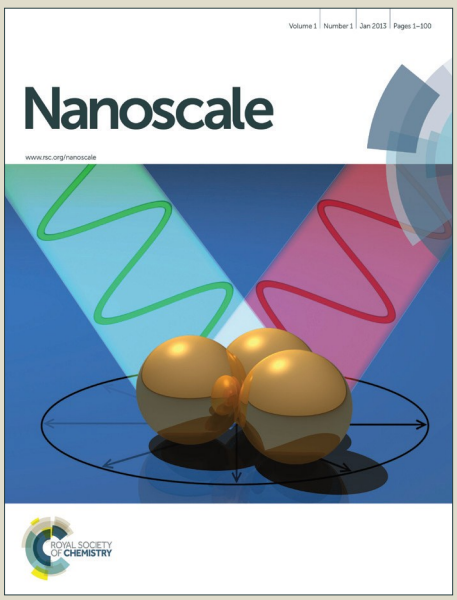

ROYAL SOCIETY OF CHEMISTRY

www.rsc.org/nanoscale

Moving graphene devices from lab to market: advanced graphene-coated nanoprobes

*Fei Hui[1], Pujashree Vajha[1], Yuanyuan Shi[1], Yanfeng Ji[1], Huiling Duan[2], Andrea Padovani[3], Luca Larcher[3], Xiao-Rong Li[4], Jing-Juan Xu[4], Mario Lanza[1]**

[1]Institute of Functional Nano & Soft Materials (FUNSOM), Soochow University, 199 Ren-Ai Road, Suzhou 215123, China. [2]State Key Laboratory for Turbulence and Complex System, Department of Mechanics and Engineering Science, CAPT, College of Engineering, Peking University, Beijing 100871, China. [3]DISMI, Università di Modena e Reggio Emilia, 42122 Reggio Emilia, Italy. [4]State Key Laboratory of Analytical Chemistry for Life Science, School of Chemistry and Chemical Engineering, Nanjing University, Nanjing 210093, China.

ABSTRACT: After more than a decade working with graphene there is still a preoccupying lack of commercial devices based on this *wonder* material. Here we report the use of high-quality solution-processed graphene sheets to fabricate ultra-sharp probes with superior performance. Nanoprobes are versatile tools used in many fields of science, but they can wear fast after some experiments, reducing the quality and increasing the cost of the research. As the market of nanoprobes is huge, providing a solution for this problem should be a priority for the nanotechnology industry. Our graphene-coated nanoprobes not only show enhanced lifetime, but also additional unique properties of graphene, such as hydrophobicity. Moreover, we have functionalized the surface of graphene to provide piezoelectric capability, and have fabricated a

nano relay. The simplicity and low cost of this method, which can be used to coat any kind of sharp tip, make it suitable for the industry, allowing production on demand.

KEYWORDS：nanoprobes, graphene, coating, atomic force microscopy, MEMS

MAIN TEXT

Graphene, a two dimensional (2D) material made of carbon atoms arranged in an hexagonal lattice, has been the focus of many theoretical studies for more than 65 years.[1] The first synthesis of graphene in 2004 opened up a new horizon in graphene and 2D materials research[2], as graphene properties could be for the first time experimentally characterized. After ten years of intensive research, graphene has shown unprecedented electronic,[2] thermal,[3] mechanical,[4] magnetic[5] and optical properties,[6] as well as other more exotic capabilities like water transparency[7] and oxidation resistance.[8] According to the last graphene roadmap[9], only in 2013 more than 16,000 research papers related to graphene were published, and to date more than 14,000 graphene patents have been registered. Nevertheless, after more than 10 years working with graphene there is still a preoccupying lack of commercial devices based on graphene.[10,11] Among the main factors hindering the use of graphene in real devices are: *i)* absence of a bandgap, which limits its use in logic applications; *ii)* lack of an industry-friendly methodology to produce graphene on insulating substrates, which is necessary to fabricate field-effect transistors, among others; *iii)* severe inhomogeneity within graphene sheets, including thickness fluctuations, lattice distortion at the domain boundaries, and dopant impurities, which produce premature device degradation;[12] *iv)* high device-to-device variability due to the presence of uncontrollable amounts of defects, which complicates the fabrication of graphene-based circuits; *v)* ageing mechanisms and progressive degradation of graphene based devices due to the effect of

the environment.[13,14] For these reasons, in 2015 graphene industry still relies on the commercialization of the raw material[15,16] and, despite graphene roadmaps predicting a great expansion around 2020,[9] to date graphene devices remain absent in the nanotechnology market.

Here we report the use of high quality solution-processed graphene sheets to enhance the performance of micro electromechanical systems (MEMS), namely ultra sharp nanoprobes. Nanoprobes are highly required in many fields of science, including physics, mechanics, microelectronics, nanotechnology, medicine and biology,[17-19] as they allow fabrication and characterization with high spatial resolution.[20-22] But, unfortunately, most nanoprobes available in the market lose their initial good performance extremely fast after some scans or spectroscopic measurements, especially during electrical or mechanical experiments.[23,24] To solve this problem, the industry has developed mainly two strategies. The first one is the use of highly stable varnishes, such as doped-diamond. This methodology effectively enhances the lifetime of the tip, but the radius and price remarkably increase[25,26] (see Supporting Information Table S1). The second is the use of bulk tips made of stable materials. Williams et al.[27] fabricated platinum wires with an apex radius below 20 nm, and IMEC (Interuniversity Microelectronics Center, Belgium) developed solid doped-diamond probes[28] that are even suitable for local etching.[29] Despite this methodology provides higher performance, the use of more expensive materials and hone techniques prohibitively increases the fabrication costs. A recent and still experimental methodology to avoid fast nanoprobe wearing is the use of graphene as protective coating. Wen *et al.*[30] grew a layer of graphene on commercial Au-varnished AFM tips by chemical vapor deposition (CVD). Martin-Olmos *et al.*[31] fabricated a similar device growing graphene in a copper mold before filling it with an SU-8 resist, and subsequently etching the copper to liberate

the graphene-coated SU-8 tip. Shim et al.[32] and Lanza et al.[33,34] reported the fabrication of graphene-coated AFM tips by transferring CVD graphene (grown on copper) onto commercial models. Although in all cases the prototypes showed enhanced performance in different applications, these fabrication methods are still far from being competitive for the industry, as they are slow and expensive, and involve human labor. Moreover, the quality of the CVD carbon film grown directly on the tip may not be as good as the one grown on copper, the use of molds remarkably increases the tip radius,[31] and transferring graphene on the tip may lead to residues of polymer on the graphene.[35]

To overcome these barriers we have fabricated graphene-coated nanoprobes by dipping standard metal-varnished AFM tips in a solution containing high quality graphene sheets. Solution-processed graphene has been successfully used to fabricate a wide range of devices, including zinc-air batteries,[36] bio-sensors,[37] and selective detectors.[38] Previous works demonstrated that even more complex nanostructures like carbon nanotubes can be successfully attached to the probes. Dai *et al.*[39] used acrylic adhesive to stick a bundle of 5-10 nanotubes to the apex of an AFM tip, leading to high aspect ratio topographic images and enhanced spatial resolution. In our case, the attachment of graphene to the nanoprobe is a much easier process: the two-dimensional sheet can perfectly follow the sharp profile of the tip, getting attached by the strong Van der Waals forces at the apex and leading to a conformal coating even for tips with different geometries. As a result, we report the cost-effective fabrication of graphene nanoprobes with superior performance and low price.

More than 20 standard metal-varnished silicon nanoprobes from different manufacturers and with different shapes and properties have been coated with graphene by immersing them in a solution containing high-quality graphene flakes. The graphene flakes powder has been prepared

from graphite by a series of redox reactions[40] (see methods section). Transmission electron microscopy (TEM) of the graphenes showed good homogeneity free of local defects, and atomic force microscopy (AFM) images revealed a flat surface free of dangling bonds and a thickness of ~0.8 nm,[40] which is close to the thickness of monolayer graphene sheets produced by this method.[41] More details about the fabrication process are given in the Supporting Information (Figures S1-S2). Figure 1 shows scanning electron microscope (SEM) images of different AFM tips coated with graphene. The graphene can effectively adapt to the sharp shape of the nanoprobes, getting attached by the high Van der Waals forces at the apex and forming a conformal coating. It is worth noting that the objective of this experiment is to ensure graphene coating at the apex, which is the only part of the nanoprobe that will get in contact with the sample, suffering large frictions during the scans and the highest current densities during electrical measurements. It is worth noting that excesses of graphene on the back side of the cantilever may affect the reflection of the AFM laser into the photodiode, especially the value of the light intensity (SUM), but in our experiments we obtained small reductions below 20%, which allows effective tip deflection detection (see Figure S1). The effectiveness of the graphene coating on the tip apex depends on different parameters such as the density and size of graphene sheets in the solvent and the geometry of the tip used, and we observe that sharper tips (Figs. 1b, 1c and 1d) may show more ideal coating compared to pyramidal tips (Fig. 1e). We are aware that this fabrication methodology may raise concerns about the number of graphene layers attached to apex of different tips. To quantify this effect, we performed an exhaustive device variability analysis (see Supporting Information Figures S3-S6 and Table S2) and conclude that the differences introduced by our coating method are much smaller than the intrinsic variability provided by the nanoprobes manufacturer. An interesting property of the graphene coating is

that, unlike other hard three-dimensional (3D) coatings (such as doped diamond),[26] the mass of graphene is almost negligible compared to that of the cantilever, which keeps unaltered its mechanical properties. We observe deviations on the resonance frequency much lower than the limits provided by the manufacturer (Figure 1f).

After corroborating conformal coating, we analyze how the presence of graphene can enhance the lifetime of the nanoprobes. To do so, we developed an accurate characterization methodology to monitor the progressive degradation of both standard and graphene-coated nanoprobes (Supporting Information Figures S7-S9), using the conductive AFM (CAFM). Our experiments demonstrate that standard nanoprobes lose their initial sharp shape and conductivity after some scans. Figure 2a shows the 1st and 13th CAFM current maps collected with a standard metal-varnished nanoprobe using a deflection setpoint of 4V and a bias of 1V (see a complete sequence of halfway scans in Supporting Information Figure S10). Both the current images and the spectra in Figure 2a, as well as the IV curves and SEM images (Figures 2b and 2c, respectively) reveal dramatic tip degradation. On the contrary, under the same testing conditions, similar tips coated with graphene show almost unaltered performance even after 92 scans (Figures 2d-f). The SEM image in Figure 2f proves that the graphene coating avoids metal-varnish melting. We statistically corroborated these observations by repeating the experiments for many standard and graphene nanoprobes, and we always observed similar results (Figure 2g). Different measuring parameters and characterization methodologies also corroborated the enhanced performance of the graphene-coated tips. We analyzed the lifetimes of graphene-coated tips under spectroscopic measurements, in which the tip remains static on the surface of the sample. Figure 2h shows the current-time (I-t) curve measured for different probe tips under a bias of 1V. It can be observed that the currents measured for the standard Pt-varnished tip rapidly decreased (after 35 s) until

reaching the noise level, showing the fast wearing of the bare Pt-varnish.[23,24] On the contrary, a similar tip coated with graphene showed high currents during the whole 1h I-t test, and the large lifetime increase in this kind of measurements, which is comparable to the performance of diamond-coated nanoprobes (Supporting Information Figures S11 and S12), which are known to be the most durable in the market. In order to prove the durability of the graphene coating we applied extraordinary high forces to a graphene coated tip, and surprisingly observed that, while the tip apex can break due to the frictions during the scan, the graphene flake effectively resisted the mechanical strain, trapping the detached particle (Figure S13). It suggests that the methodology could be used in the future to intentionally trap particles or fluids between the tip and graphene sheet and test their mechanical properties.

In addition to the inexpensive enhancement of lifetime, graphene can also provide additional and unprecedented capabilities to the nanoprobes. For example, it is widely known that the effect of relative humidity can alter the data collected in experiments performed under room atmosphere, increasing the effective areas under test[42] and producing undesired chemical reactions such as local anodic oxidation[43] (among others). Therefore, the use of highly hydrophobic nanoprobes would be interesting in a wide range of applications, as they can repel water molecules from the tip/sample junction; but unfortunately, conductive metal-varnished nanoprobes are always highly hydrophilic. One solution could be using hydrophobic and conductive polymer coatings,[44] but their 3D nature would unavoidably produce a prohibitive increase of the tip radius and loss of lateral resolution (Supporting Information Figure S14). In this direction, we prove that the highly hydrophobic nature of the 2D graphene coating can be an excellent alternative. Figure 3a shows the typical forward and backward I-V curves collected with standard and graphene nanoprobes

on a piece of n-type silicon. The standard tip shows an initial large and unreal resistance related to the presence of water molecules between the tip and the sample (Figure 3c), which introduce a potential barrier. When the voltage increases, a shift is observed in the backward curve, indicating that the water barrier has been perforated due to the larger tip/sample contact force provoked by the voltage applied, as shown in Eq. 1:[45-47]

$$F_C = K \cdot \delta + F_{EL} + F_{WM} + F_{VW} + F_{OTHERS} \qquad \text{(Eq.1)}$$

where F_C is the tip/sample contact force, F_{EL} is the electrostatic force (which depends on the voltage applied), F_{WM} is the anti-repulsive force created by the water meniscus, F_{VW} are the Van der Waals forces (which are negligible compared to the others) and F_{OTHERS} are less relevant contributions from external factors. After water layer removal, the measured I-V curve reveals the real current values through the silicon sample as previously observed in the literature.[48] On the contrary, graphene-coated nanoprobes show real characterization in both forward and backward curves, indicating that no water barrier has formed between the tip and the sample (Figure 3d), due to the highly hydrophobic nature of graphene. Interestingly, the initial I-V curve measured with standard tips (which is the only one in which the water barrier is present) shows a sharp current increase, due to the sudden breakdown of the barrier, while all other plots show typical Schottky conduction typical of silicon samples. Such resistance switch behavior is corroborated by tunnel current modeling (see black lines in Figure 3b and Figure S15). Basically a squared Pt/H_2O/Si heterojunction has been simulated to match the typical tip/sample contact area for an AFM working condition, and previously reported values for the work function of Pt, the affinity of the water layer and its dielectric constant have been applied to calculate the current flow between the tip and the sample (see also supplementary information). The results indicate that the water barrier between the tip and the sample for the trace and retrace plots is 10 Å and 1

Å, respectively. This result is supported by comparing 100 backward I-V curves collected with both standard and graphene-coated nanoprobes. As Figures 3e and 3f show, the onset voltage of the graphene nanoprobes is smaller, probably due to the different work functions between the Pt and graphene tip electrodes. More importantly, the variability of the I-V curves registered is lower for the graphene nanoprobes, due to a better and more stable contact in the absence of water. Further hydrophobicity analyses (not shown) indicate that the adhesion force measured in distance (F-d) curves is smaller using graphene-coated tips. It also indicates that the water layer is removed, and the total force is reduced by the elimination of the term F_{WM} in Eq. 1.

Finally, we demonstrate that as the surface of graphene can be engineered, the properties of graphene-coated nanoprobes can be easily tuned. For example, graphene is known to be a non-piezoelectric material but when doped with specific species such as Li, K, H or F, piezoelectric effects can be introduced by breaking inversion symmetry.[49] Such behavior has been only theoretically predicted but never experimentally demonstrated. In the following experiments, we have coated standard nanoprobes using normal and K-modified graphene sheets (similar to those reported in our previous work[40]), and take advantage of the engineered piezoelectricity in graphene sheets to fabricate a nano relay. The K-doped graphene flakes deposited on the cantilever of the nanoprobe have been stretched by means of F-d curves (see Figure 4a), and the current has been simultaneously monitored using an absolute bias of 0V (see Supporting Information Figure S16). Figure 4b shows the different contact cycles collected using a nanoprobe coated with K-modified graphene. As can be observed, without the application of any bias, the deflection of the cantilever is accompanied by a generation of a current pulse, similar to that reported for other piezoelectric nanostructures.[50,51] Figures 4c and 4d reveal the correlation between the force and current signal, which can be divided in three regions: cut-off, quasi-linear

(with a slope of ~ 70 pA/nN), and saturation. We repeated these experiments for the standard tips coated with undoped graphene, but observed no signs of current, indicating that the piezoelectric current should be provided by the K-doping, in agreement with previous predictions. [49,52] We repeated the experiments using nanoprobes coated with thin flakes of multilayer MoS_2 (which is a 2D material known to be piezoelectric[52]) but again no current signals have been observed. Interestingly, Reed and co-workers[49,52] reported that, while in-plane piezoelectric potential is induced in strained MoS_2 fields, in K-modified graphene the potential appears perpendicular to the graphene sheet. Therefore, the piezoelectric potentials in the MoS_2 sheets may be short-circuited by the underlying metallic varnish of the tip, while the K-modified graphene sheet produced a net transversal current flow.

The fact that the current in our device increases linearly vs. the applied force and strain (Figure 4d) further supports this hypothesis, because the piezoelectric potentials observed experimentally in other materials[53,54] and theoretically predicted for K-modified graphene[49] also increase linearly. Figure 4c further reveals that the current does not increase immediately when the tip contacts the surface of the sample, but it requires a minimum contact force (strain) to generate the current (F_{ON}). This observation shows that the current does not come from any parasitic voltage source, such as electrical noise or offsets. Actually, if that would be the case, the current should have increased exponentially with the contact force, according to equations (1) and (3) in the Supporting Information. Moreover, F_{ON} indicates the presence of an initial Schottky barrier,[55] which is fully eliminated with the generated piezoelectric potential. Finally, the saturation region reveals that the internal electrical field cannot further increase, as previously observed for GaN and other piezoelectric materials,[53,54] probably due to the saturated rotation of

electric dipoles. The simplicity of our fabrication methodology and current observation contrast with the complex setups developed for the observation of piezoelectricity in MoS_2,[56,57] which also depend on thickness fluctuations and atomic orientation, both of them are very difficult to control. We have fabricated 14 different nano relays based on nanoprobes coated with K-modified graphene, and 88% of the current-distance curves collected showed reproducible current peaks as those shown in Figure 4b, while uncoated nanoprobes and nanoprobes coated with undoped graphene or MoS_2 did not show signals of currents in unbiased experiments. This behavior can be useful for a wide range of applications, including proximity sensors, nano switches and nano relays.[58]

In summary, we have developed an inexpensive methodology to fabricate graphene-coated nanoprobes with lifetimes much longer than the uncoated counterparts and performance better than most stable commercial nanoprobes. Further, graphene nanoprobes show interesting additional capabilities, such as: i) hydrophobicity, which results in a better and more stable tip/sample contact in the absence of water meniscus; and ii) piezoelectricity (using K-modified graphene sheets), which has been used to simulate a nano relay. The present coating method is fast, inexpensive, and compatible with industrial production.

METHODS

Graphene solution preparation: The graphene sheets were synthesized from graphite by a series of redox reactions. Graphite powder (2 g), H_2SO_4 (12 mL), $K_2S_2O_8$ (3.0 g) and P_2O_5 (3.0 g) were mixed at 80 ºC for 5 h, diluted in 500 mL pure water, filtered and reoxidized by Hummers and Offeman method. The resulting product was mixed with 150 mL H_2SO_4 at 0 ºC and 25 g $KMnO_4$ were added under stirring at around 5 ºC. The mixture was agitated for 4 h, diluted in 1,250 mL pure water and 30% H_2O_2, washed in 1:10 HCl and pure water, and dried naturally.

Finally, it was purified by dialysis for 1 week and exfoliated by sonicating 0.1 mg/mL. Graphene oxide reduction consisted of adding 5 ml Hydration Hydrazine into 50 mL solution of 0.1 mg/mL, stirring for 24 h at 80 ºC. Finally, black powder graphene was obtained by filtering the product and drying in vacuum. More details about the synthesis of graphene are provided in our previous report (reference 40 in the manuscript). The graphene solution was prepared by mixing 5 mg of graphene powder and 1 mL of pure water, and the solution was sonicated at 50 W for 10 min. The thickness of the graphene sheets in solution was measured to be about 0.7 nm, which is close to that of a single layer graphene sheet, and their size is less than 1µm.

Fabrication of graphene coated AFM tips: In this investigation, we used four different types of standard AFM nanoprobes: i) Silicon tips varnished with 20 nm Pt from Olympus (model OMCL-AC240-TM, item no. 2C071D). The theoretical resonance frequency and spring constant provided by the manufacturer are 70 kHz and 2 N/m, with a ± 20% allowed deviation. ii) Silicon tips varnished with Pt-Ir from Bruker (model SCM-PIC, item no. A008/01). The theoretical resonance frequency and spring constant provided by the manufacturer are 13 kHz and 0.2 N/m, with a ± 23% allowed deviation. iii) Silicon tips varnished with 20 nm Pt from Bruker (model OSCM-PT-R3, item no. 131301). The theoretical resonance frequency and spring constant provided by the manufacturer are 70 kHz and 2 N/m, with a ± 28% allowed deviation. iv) Silicon tips varnished with 100 nm doped diamond from Bruker (model DDESP-FM-10, item no. 71109L856). The theoretical resonance frequency and spring constant provided by the manufacturer are 80 kHz and 3 N/m, with a ± 25% allowed deviation. We immersed the as-received metal-varnished nanoprobes in the graphene solution for 1 minute, and after that the tips were dried by blowing N_2 on them. The graphene sheets easily attached to the sharp apex of the

AFM tip by Van Der Waals forces, leading to a conformal coating. The use of N_2 enhances the adhesion between the graphene and the tip apex. The amount of graphene sheets on the tip can be controlled by tuning the concentration of graphene in solution (see next section).

Characterization: The electrical properties of standard and graphene-coated tips were studied with a Veeco Multimode V CAFM by means of I-V curves and topography/current maps. The scanned samples consisted of monolayer graphene/Cu stacks purchased form ACS Materials (item no. XF013). The characterization of the tips has been made following a three steps process, as detailed in Figure S3. Basically, it consists of: i) characterization of the tip by means of I-V curves; ii) degradation of the tip by sequences of current maps; and iii) characterization of the tip. The parameters were tuned before the experiments, and the best imaging conditions in lateral scans were obtained for a bias of 1V and a deflection setpoint of 4V. All CAFM images were analyzed offline with the Nanoscope Analysis software (version 1.4) from Bruker. For the I-t curves, a Keithley 2400 sourcemeter was connected to the AFM tip and sample holder,[21] and remotely controlled with a custom-made Labview application. This methodology allows visualizing larger currents: the I-V curves collected with the standard CAFM saturate at 5 nA, while the sourcemeter allows monitoring large currents up to miliamperes. Before and after the CAFM tests, SEM images of all tips were collected with a Quanta 200FEG SEM using a beam intensity signal of 30 kV and a Zeiss Supra 55 SEM using a beam intensity signal of 10 kV.

We would like to highlight that all the CAFM experiments here presented have been performed in air and, for the voltages applied (up to ±10V) and the currents measured (up to ±1mA), we never observed indications of chemical reactions at the tip/sample nanojunction. We carefully

analyzed all the measurements, and we never observed oxidation/reduction current peaks or typical hillock formation related to surface modification when a chemical reaction takes place between the tip and the sample. We have repeated some of these measurements using a Seiko 3800N AFM working in a vacuum of 3·10-6 torr, and we only observed minor differences related to the lateral resolution of the technique. The fact that our experiments are reproducible in ambient conditions gives our findings even more relevance, as most of AFM work in air, implying that our nanoprobes could be used for many different experiments.

ACKNOWLEDGMENT

This work has been partially supported by the Young 973 National Program of the Chinese Ministry of Science and Technology (grant no. 2015CB932700), the Major State Basic Research Development Program of China (grant no. 2011CB013101) and the National Natural Science Foundation of China (grant no. 11225208, 11172001, 10872003, 10932001 and 11072230). The Project Funded by the Priority Academic Program Development of Jiangsu Higher Education Institutions (PAPD) is also acknowleged. Professor Mario Lanza acknowledges generous start-up funding from Soochow University and from the "Young 1000 Talent Program" of China.

REFERENCES

(1) Wallace, P. R. *Phys. Rev.* **1947**, *71*, 622.

(2) Novoselov, K. S.; Geim, A. K.; Morozov, S. V.; Jiang, D.; Zhang, Y.; Dubonos, S. V.; Grigorieva, I. V.; Firsov, A. A. *Science* **2004**, *306*, 666.

(3) Balandin, A. A.; Ghosh, S.; Bao, W. Z.; Calizo, I.; Teweldebrhan, D.; Miao, F.; Lau, C. N. *Nano Lett.* **2008**, *8*, 902.

(4) Lee, C. G.; Wei, X. D.; Kysar, J. W.; Hone, J. *Science* **2008**, *321*, 385.

(5) Tombros, N.; Jozsa, C.; Popinciuc, M.; Jonkman, H. T.; van Wees, B. J. *Nature* **2007**, *448*, 571.

(6) Bonaccorso, F.; Sun, Z.; Hasan, T.; Ferrari, A. C. *Nat. Photonics* **2010**, *4*, 611.

(7) Rafiee, J.; Mi, X.; Gullapalli, H.; Thomas, A. V.; Yavari, F.; Shi, Y. F.; Ajayan, P. M.; Koratkar, N. A. *Nat. Mater.* **2012**, *11*, 217.

(8) Chen, S. S.; Brown, L.; Levendorf, M.; Cai, W. W.; Ju, S. Y.; Edgeworth, J.; Li, X. S.; Magnuson, C. W.; Velamakanni, A.; Piner, R. D. *ACS Nano* **2011**, *5*, 1321.

(9) Novoselov, K. S.; Fal'ko, V. I.; Colombo, L.; Gellert, P. R.; Schwab, M. G.; Kim, K. *Nature* **2012**, *490*, 192.

(10) Peplow, M. *Nature*, **2013**, *503*, 327.

(11) Novoselov, K. S. *Nature*, **2014**, *505*, 291.

(12) Xu, G. Y.; Zhang, Y. G.; Duan, X. F.; Balandin, A. A.; Wang, K. L. *Proceeding of the IEEEE* **2013**, *101*, 1670.

(13) Lanza, M.; Wang, Y.; Gao, T.; Bayerl, A.; Porti, M.; Nafria, M.; Zhou, Y. B.; Jing, G. Y.; Zhang, Y. F.; Liu, Z. F.; Yu, D. P.; Duan, H. L. *Nano Reseaarch* **2013**, *6*, 485.

(14) Shi, Y. Y.; Ji, Y. F.; Hui, F.; Wu, H. H; Lanza, M. *Nano Research* **2014**, *7*, 1820.

(15) www.acsmaterial.com

(16) www.graphenea.net

(17) Lee, C.; Wei, X. D.; Kysar, J. W.; Hone, J. *Science* **2008**, *321*, 385.

(18) Longo, G.; Alonso-Sarduy, L.; Rio, L. M.; Bizzini, A.; Trampuz, A.; Notz, J.; Dietler, G.; Kasas, S. *Nat. Nanotechnol.* **2013**, *8*, 552.

(19) Chen, C. H.; Lin, C. T.; Hsu, W. L.; Chang, Y.C.; Teh, S. R.; Li, L. J.; Yao, D. *J. Nanomed. Nanotechnol.* **2013**, *9*, 600.

(20) Wei, Z. Q.; Wang, D. B.; Kim, S.; Kim, S. Y.; Hu, Y. K.; Yakes, M. K.; Laracuente, A. R.; Dai, Z. T.; Marder, S. R. Berger, C. *Science* **2010**, *328*, 1373.

(21) Garcia, R.; Herruzo, E. T. *Nat. Nanotechnol.* **2012**, *7*, 217.

(22) Hong, S. S.; Cha, J. J. Cui, Y. *Nano Lett.* **2011**, *11*, 231.

(23) Chung, K. H. *Int. J. Precis. Eng. Man.* **2014**, *15*, 2219.

(24) Vahdat, V.; Ryan, K. E.; Keating, P. L.; Jiang, Y. J.; Adiga, S. P.; Schal, J. D.; Turner, K. T.; Harrison, J. A.; Carpick, R. W. *ACS Nano* **2014**, *8*, 7027.

(25) Gozen, B. A.; Ozdoganlar, O. B. *Wear* **2014**, *317*, 39.

(26) Smirnov, W.; Kriele, A.; Hoffmann, R.; Sillero, E.; Hees, J.; William, O. A.; Yang, N. J.; Kranz, C.; Nebel. C. E. *Anal. Chem.* **2011**, *83*, 4936.

(27) Bussmann, E.; Williams, C. C. *Rev. Sci. Inst.* **2004**, *75*, 422.

(28) Hantschel, T.; Demeulemeester, C.; Eyben, P.; Schulz, V.; Richard, O.; Bender, H.; Vandervorst, W. *Phys. Status Solidi A* **2009**, *206*, 2077.

(29) Celano, U.; Goux, L.; Belmonte, A.; Opsomer, K.; Franquet, A.; Schulze, A.; Detavernier, C.; Richard, O.; Bender, H.; Jurczak, M. *Nano Lett.* **2014**, *14*, 2401.

(30) Wen, Y. G. *Adv. Mater.* **2012**, *24*, 3482.

(31) Martin-Olmos, C.; Rasool, H. M.; Weiller, B. H.; Gimzewski, J. K. *ACS. Nano.* **2013**, *7*, 4164.

(32) Shim, W.; Brown, K. A.; Zhou, X. Z.; Rasin, B.; Liao, X.; Mirkin, C. A. *Proc. Natl. Acad. Sci. U. S. A.* **2012**, *109*, 18312.

(33) Lanza, M.; Bayerl, A.; Gao, T.; Porti, M.; Nafria, M.; Jing, G. Y.; Zhang, Y. F.; Liu, Z. F.; Duan, H. L. *Adv. Mater.* **2013**, *25*, 1440.

(34) Lanza, M.; Gao, T.; Yin, Z. X.; Zhang, Y. F.; Liu, Z. F.; Tong, Y. Z.; Shen, Z. Y.; Duan, H. L. *Nanoscale* **2013**, *5*, 10816.

(35) Suk, J. W.; Kitt, A.; Magnuson, C. W.; Hao, Y. F.; Ahmed, S.; An, J. H.; Swan, A. K.; Goldberg, B. B.; Ruoff, R. S. *ACS Nano* **2011**, *5*, 6916.

(36) Li, Y. G.; Gong, M.; Liang, Y. Y.; Feng, J.; Kim, J. E.; Wang, H. L. Hong, G. S.; Zhang, B.; Dai, H. J. *Nat. Commun.* **2013**, *4*, 1805.

(37) Lu, X. B.; Wang, X.; Jin, J.; Zhang, Q.; Chen, J. P. *Biosens. Bioelectron* **2014**, *62*, 134.

(38) Li, X. R.; Kong, F. Y.; Liu, J.; Liang, T. M.; Xu, J. J.; Chen, H. Y. *Adv. Funct. Mater*. *2012*, *22*, 1981.

(39) Dai, H. J.; Hafner, J. H.; Rinzler, A. G.; Colbert, D.T.; Smalley, R. E. *Nature* **1996**, *384*, 147.

(40) Li, X. R.; Kong, F. Y.; Liu, J.; Liang, T. M.; Xu, J. J.; Chen, H. Y. *Adv. Funct. Mater.* **2012**, *22*, 1981.

(41) Li, D.; Muller, M. B.; Kaner, R. B.; Wallace, G. G. *Nat. Nanotechnol.* **2008**, *3*, 101.

(42) Lanza, M.; Nafria, M.; Aymerich, X.; Whittaker, E.; Hamilton, B. *Rev. Sci. Instrum.* **2010**, *81*, 106110.

(43) Garcia, R.; Martinez, R. V.; Martinez, J. *Chem. Soc. Rev.* **2006**, *35*, 29.

(44) Dong, Y. F.; Liu, S. H.; Wang, Z. Y.; Liu, Y.; Zhao, Z. B.; Qiu, J. S. *Nanoscale* **2015**, *7*, 7569.

(45) Israelachvili J. N. *Academic Press*, London, **1992**.

(46) Frammelsberger, W.; Benstetter, G.; Kiely, J.; Stamp, R. *Appl. Surf. Sci.* **2006**, *252*, 2375.

(47) Frammelsberger, W.; Benstetter, G.; Kiely, J.; Stamp, R. *Appl. Surf. Sci.* **2007**, *253*, 3615.

(48) Blasco, X.; Nafria, M.; Aymerich, X. *Surf. Sci.* **2003**, *532*, 732.

(49) Ong, M. T.; Reed, E. J. *ACS Nano* **2012**, *6*, 1378.

(50) Xu, X.; Potie, A.; Songmuang, R.; Lee, J. W.; Bercu, B.; Baron, T.; Salem, B.; Montes, L. *Nanotechnology* **2011**, *22*, 105704.

(51) Zhou, Y. S.; Hinchet, R.; Yang, Y.; Ardila, G.; Songmuang, R.; Zhang, F.; Zhang, Y.; Han, W. H.; Pradel, K.; Montes, L.; Mouis, M.; Wang, Z. L. *Adv. Mater.* **2013**, *25*, 883.

(52) Duerloo, K. A. N.; Ong, M. T.; Reed, E. J. *J. Phys. Chem. Lett.* **2012**, *3*, 2871.

(53) Kang, M. G.; Oh, S. M.; Jung, W. S.; Moon, H. G.; Baek, S. H.; Nahm, S.; Yoon, S. J.; Kang, C. Y. *Sci. Rep.* **2015**, *5*, 10151.

(54) Alam, M. M.; Ghosh, S. K.; Sultana, A.; Mandal, D. *Nanotechnology* **2015**, *26*, 165403.

(55) Li, Z.; Ezhilarasu, G.; Chatzakis. L.; Dhall, R.; Chen, C. C.; Cronin, S. B. *Nano Lett.* **2015**, *15*, 3977.

(56) Wu, W. Z.; Wang, L.; Li, Y. L.; Zhang, F.; Lin, L.; Niu, S. M.; Chenet, D.; Zhang, X.; Hao, Y. F.; Heinz, T. F.; Hone, J.; Wang, Z. L. *Nature* **2014**, *23*, 470.

(57) Zhu, H. Y.; Wang, Y.; Xiao, J.; Liu, M.; Xiong, S. M.; Wong, Z. J.; Ye, Z. L.; Ye, Y.; Yin, X. B.; Zhang, X. *Nat. Nanotechnol.* **2015**, *10*, 151.

(58) Hinchet, R.; Montes, L.; Bouteloup, G.; Ardila, G.; Parsa, R.; Akarvardar, K.; Howe, R. T.; Philip Wong, H. –S. *DTIP* Aix-en-Provence, France, **2011**.

FIGURES

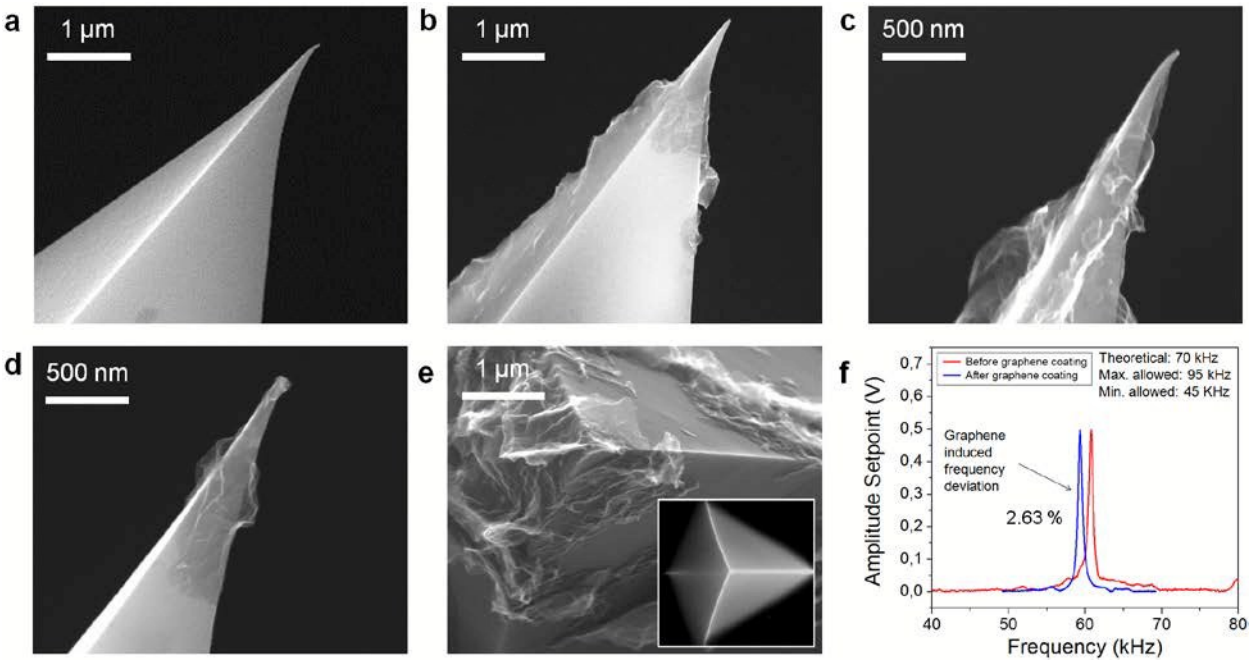

Figure 1. Coating standard nanoprobes with graphene sheets. SEM images of different Pt-varnished silicon tips before and after graphene coating. (a) As-received OMCL-AC240 nanoprobe; (b,c) OMCL-AC240 nanoprobes coated with low and high density of graphene sheets (respectively); (d,e) OSCM-PT and SCM-PIC nanoprobes coated with low density of graphene sheets (respectively). The inset in (e) shows the corresponding uncoated model. Conformal graphene-coating has been successfully achieved for nanoprobes with different geometries. (f) Resonance frequency measured with the AFM in tapping mode before and after coating an OMCL-AC240 nanoprobe with graphene.

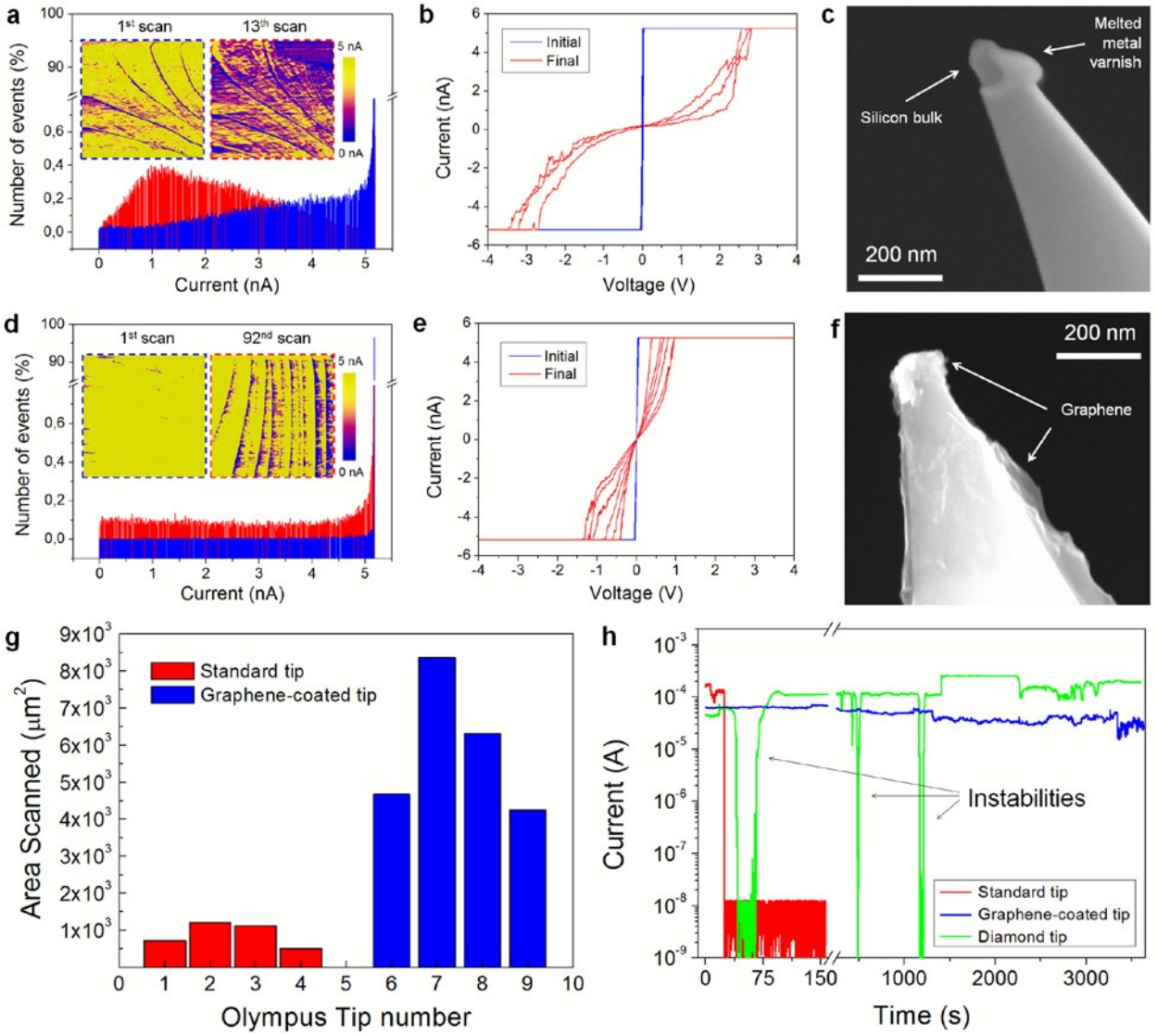

Figure 2. Lifetime characterization of graphene coated nanoprobes. The insets in (a) are 1st and 13th CAFM current maps collected with a standard metal-varnished nanoprobe. Both the current images (insets) and the spectra in (a), as well as the IV curves (b) and SEM images (c) reveal dramatic tip degradation. Under the same testing conditions, similar tips coated with graphene show almost unaltered performance even after 92 scans (d-f). (g) Comparative plot showing the maximum areas scanned with standard and graphene-coated nanoprobes before observing any signal of yield decrease. (h) I-t curves measured for the probes without (red) and with (blue) graphene coating. The doped diamond varnished tip (green) is plotted as reference.

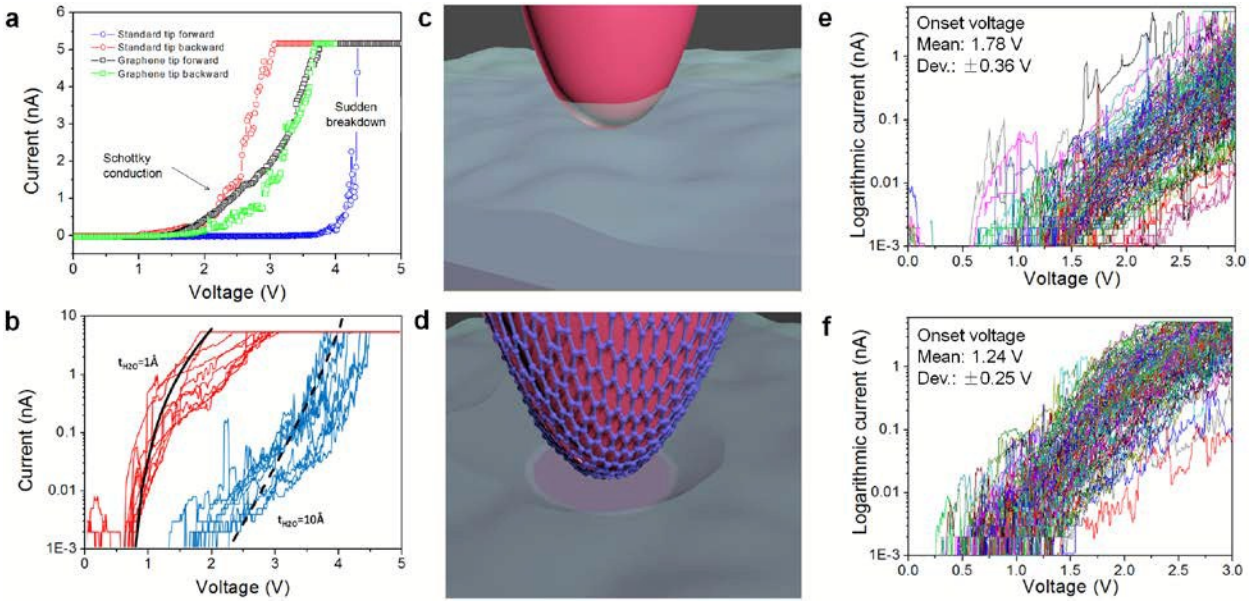

Figure 3. Hydrophobic characterization of graphene nanoprobes. (a) typical forward and backward IV cures collected with standard and graphene nanoprobes on a piece of n-type silicon. (b) Fitting of the forward and backward IV curves collected with the standard tip to the charge transport model (see details in the Supporting information). The forward plot fits for a water barrier of 10 Å, while the backward does for 1 Å. 3D schematics of (c) standard and (d) graphene nanoprobe, which shows the water resistance of graphene. 100 backward IV curves collected with both standard (e) and graphene-coated nanoprobes (f), the onset voltage and the deviation of the graphene nanoprobes is much smaller.

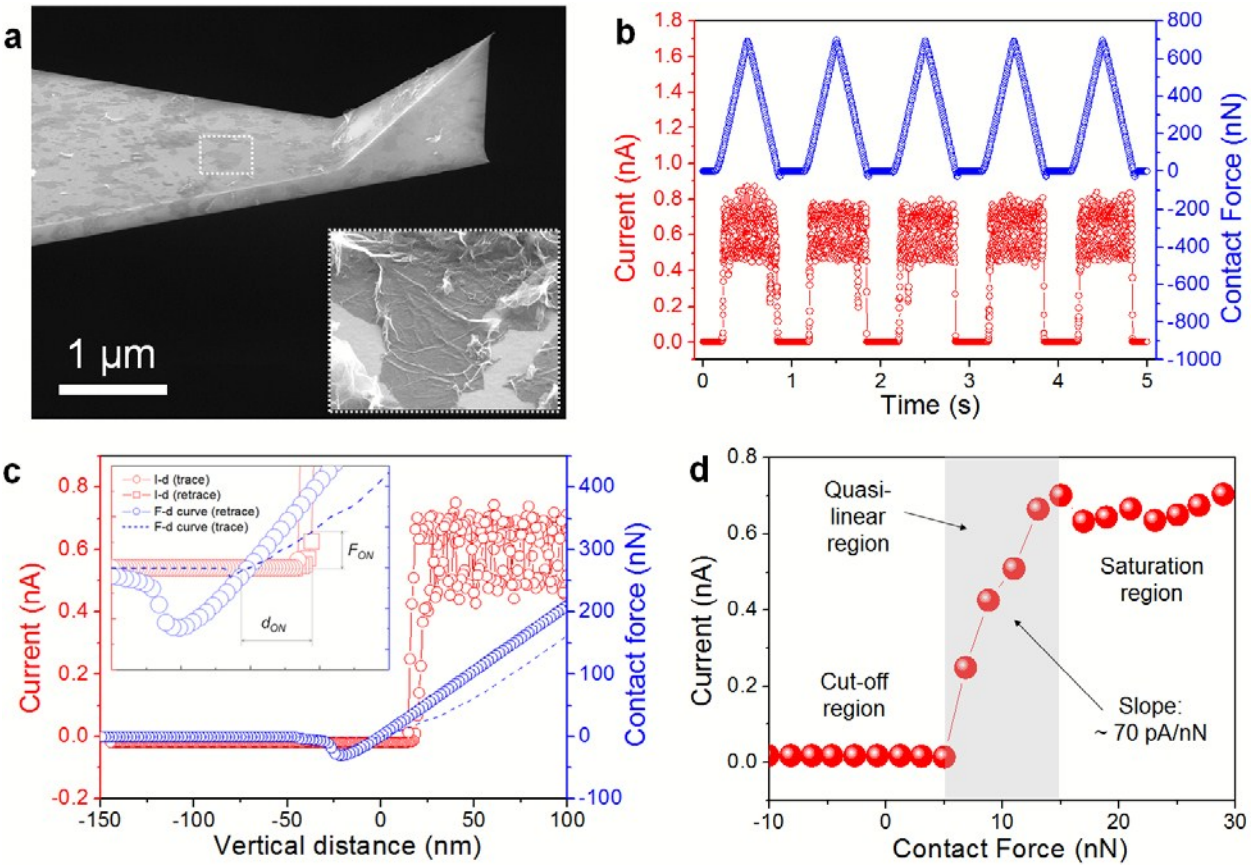

Figure 4. Piezoelectric measurements of K-doped graphene based on nanoprobes. (a) SEM image of an nanoprobe with the cantilever partially coated with graphene. (b) shows the different contact cycles collected with a nanoprobe coated with K-doped graphene. (c) and (d) reveal the correlation between the force and current signal, which can be divided in three regions: cut-off, quasi-linear and saturation. Inset in (c) is the zoom-in region of a minimum contact force (strain) (F_{ON}) and minimum distance (d_{ON}) to generate the current.